

# Synthesis, properties, and dehydroxylation of members of the crandallite-goyazite series

R. J. GILKES AND B. PALMER

Department of Soil Science and Plant Nutrition, University of Western Australia, Nedlands,  
Western Australia, 6009, Australia

**ABSTRACT.** Unit-cell parameters of synthesized members of the crandallite ( $a = 7.007 \text{ \AA}$ ,  $c = 16.216 \text{ \AA}$ )-goyazite ( $a = 7.013 \text{ \AA}$ ,  $c = 16.650 \text{ \AA}$ ) series vary linearly with composition between end-members. Most members of the series consist of  $0.1 \mu\text{m}$  platy crystals, but crandallite also contains some larger ( $1\text{--}5 \mu\text{m}$ ) tapered crystals elongated along the  $c$  axis.

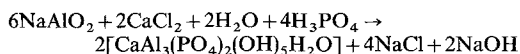
With increasing Sr substitution the dehydroxylation temperature decreases from  $c. 475^\circ\text{C}$  for crandallite to  $420^\circ\text{C}$  at 20 mole % Sr, and then increases to  $440^\circ\text{C}$  for goyazite. Partial dehydroxylation of crandallite is accompanied by contraction of the  $c$  unit cell parameter and expansion of  $a$ , thereby retaining an unaltered unit cell volume. The much greater sensitivity of  $c$  to both Sr substitution and dehydroxylation may be due to the rigidity of continuous sheets of  $\text{Al}(\text{OH})_4\text{O}_2$  octahedra which are parallel to the (001) plane in these minerals.

MINERALS of the plumbogummite series  $[(\text{Ca}, \text{Sr}, \text{Pb}, \text{Ba}, \text{RE})\text{Al}_3(\text{PO}_4)_2(\text{OH})_5 \cdot \text{H}_2\text{O}]$  have been intensively studied by soil scientists in recent years since they may be a significant site of soil phosphorus (Norrish, 1968) and because minerals with compositions similar to the Ca-rich member crandallite are used as fertilizers (Doak *et al.*, 1965; Hoare, 1980). Their effectiveness as fertilizers is greatly improved by calcination at temperatures between  $450$  and  $650^\circ\text{C}$  to produce an amorphous dehydroxylated residue (Hill *et al.*, 1950; Gilkes and Palmer, 1979). The optimum calcination temperature may depend on the chemical composition of the mineral, since published thermal analyses indicate that the dehydroxylation temperature of plumbogummite-group minerals is quite sensitive to composition, varying in the range  $400\text{--}655^\circ\text{C}$  (Table I).

This paper examines the effect of chemical composition on the unit cell parameters and dehydroxylation behaviour of synthetic members of the crandallite (Ca)-goyazite(Sr) series. Other plumbogummite minerals were not investigated since only Sr substituted crandallite is used to produce commercial fertilizers (Gilkes and Palmer, 1979; Hoare, 1980).

## Materials and methods

The method of synthesis used was that described by Slade (1974) which was in turn based on the work of Ignatova *et al.* (1965). The reaction is:



Members of the isomorphous series crandallite  $[\text{CaAl}_3(\text{PO}_4)_2(\text{OH})_5 \cdot \text{H}_2\text{O}]$  to goyazite  $[\text{SrAl}_3(\text{PO}_4)_2(\text{OH})_5 \cdot \text{H}_2\text{O}]$  were prepared by substituting various amounts of  $\text{SrCl}_2$  for  $\text{CaCl}_2$ . The resultant gels were crystallized in a stainless steel pressure vessel with a glass insert for two weeks at  $200^\circ\text{C}$  and  $1.5 \times 10^6 \text{ Nm}^{-2}$ .

X-ray powder diffraction patterns were obtained with a Philips vertical goniometer with graphite-monochromatized  $\text{Cu-K}\alpha$  radiation and scan speed of  $0.125^\circ/20/\text{min}$ . using a quartz internal standard.

Transmission electron micrographs (TEM) were obtained with a Hitachi HU11 instrument. Selected area electron diffraction (SAD) patterns were calibrated for spacing measurements with evaporated gold and for rotation measurements with  $\text{MoO}_3$  crystals (Gard, 1971). Scanning electron micrographs were obtained on a Philips PSEM 500 instrument on gold-coated specimens.

Thermogravimetric (TGA) and differentiated thermogravimetric curves (DTGA) were obtained on 10 mg samples in flowing air at a heating rate of  $10^\circ\text{C}/\text{minute}$  using a Perkin Elmer TGS2 instrument, and DTA curves on 100 mg samples using a Stanton 673 instrument with the same conditions.

## Results and discussion

**X-ray diffraction.** Crandallite-goyazite minerals were major constituents of all preparations. Minor amounts of boehmite and various strontium-substituted hydroxyapatites were also found to be present. Because of the uncertain assignments of several reflections, unit cell dimensions for the crandallite-goyazite series (fig. 1) were determined solely from  $d$  values of the strong, well-resolved 303 and 220 reflections rather than by least squares calculations based on many reflections. This procedure was also adopted by McKie (1962) in his study of naturally occurring members of the

TABLE I. *Dehydroxylation temperatures of plumbogummite-group minerals*

Mineral	Dehydroxylation temperature (°C)†	Reference
Cr <sub>8</sub> Fc <sub>39</sub> Go <sub>48</sub> Gx <sub>6</sub> *	636, 655	McKie (1962)
Cr <sub>13</sub> Fc <sub>48</sub> Go <sub>39</sub> Gx <sub>0</sub>	628	McKie (1962)
Gorceixite	495, 550	Ankinowitch and Silantjewa (1959)
Gorceixite	520	Rao (1966)
Cr <sub>6</sub> Fc <sub>0</sub> Go <sub>3</sub> Gx <sub>91</sub>	580	Nicolas and de Rosen (1963)
Cr <sub>6</sub> Fc <sub>0</sub> Go <sub>3</sub> Gx <sub>91</sub>	500–700	Povondra and Slansky (1966)
Crandallite	400	Hill <i>et al.</i> (1950)
Crandallite	450	Gilkes and Palmer (1979)
Crandallite	475	Doak <i>et al.</i> (1965)
Crandallite	512	Cowgill <i>et al.</i> (1963)
Crandallite	530	Blanchard (1972)

\* Cr—crandallite; Fc—florencite; Go—goyazite; Gx—gorceixite. Compositions are mostly approximate and the examples of gorceixite and crandallite are not true end-members as they exhibit significant substitutions.

† Approximate temperatures in some instances as DTA or DTGA peaks were partially obscured by dehydroxylation peaks of clay and other minerals.

plumbogummite group. The *c*-axis dimension increased linearly with molar % Sr in the original gel and the *a*-axis dimension also increased slightly. The values of *a* = 7.007 Å, *c* = 16.216 Å for crandallite agree well with published data (Table II). The *c*-axis dimension of goyazite is substantially higher than published values for natural goyazite (Table II). This discrepancy is probably due to the substantial isomorphous substitution of Ca and other ions in natural goyazite specimens.

McKie (1962), on the basis of his study of

TABLE II. *Unit cell dimensions of crandallite and goyazite*

<i>a</i> (Å)	<i>c</i> (Å)	Reference
<i>Synthetic crandallite</i>		
7.007	16.216	This work
6.989	16.159	Slade (1974)
<i>Natural crandallite</i>		
7.005	16.192	Blount (1974)
7.003	16.166	Radoslovich (1969)
7.013	16.196	Blanchard (1972)
7.000	16.194	Mitchell and Knowlton (1971)
7.005	16.192	Palmer (1979)
<i>Synthetic goyazite</i>		
7.013	16.650	This work
<i>Natural goyazite</i>		
7.021	16.505	Kato and Radoslovich (1968)
6.981	16.487	Guillemin (1955)
6.982	16.540	McKie (1962)

naturally-occurring members of the plumbogummite group, showed that both the *a* and *c* unit-cell dimensions increased linearly with the average effective radius of the large cations (e.g. Ba, Pb, Ca, Sr). The straight line relationships derived by McKie have been adapted to the crandallite-goyazite series and are plotted in fig. 1. The predicted slopes and values of the *a* and *c* axes for end-members are different from those which we have obtained. This discrepancy is probably mainly due to McKie's data having been derived exclusively from low-Ca specimens (no crandallite or near-crandallite specimens were included in his study), so that his linear relationships predict much lower values of *a* and *c* for crandallite than are observed (i.e. 6.927, 16.005 Å compared to 7.007, 16.216 Å respectively).

The differences between the unit-cell dimensions of crandallite-rich members of the crandallite-goyazite series and those values predicted by McKie's relationships may be due to the small size of the Ca ion (*r* = 0.99 Å) relative to the size of the twelvefold co-ordinated site which it occupies. The other cations that may occupy this site are much larger than Ca (Ce 1.16, Sr 1.13, Pb 1.20, Ba 1.35 Å) and may protrude more from within the co-ordinating anion sheets, as is discussed by McKie (1962) and Kato and Radoslovich (1968). The relative invariance of the *a* axis compared to the *c* axis indicates a greater rigidity within the (001) plane, so that substitutions of large cations are mostly accommodated by expansion in the *c* direction. The continuous sheets of Al(OH)<sub>4</sub>O<sub>2</sub>

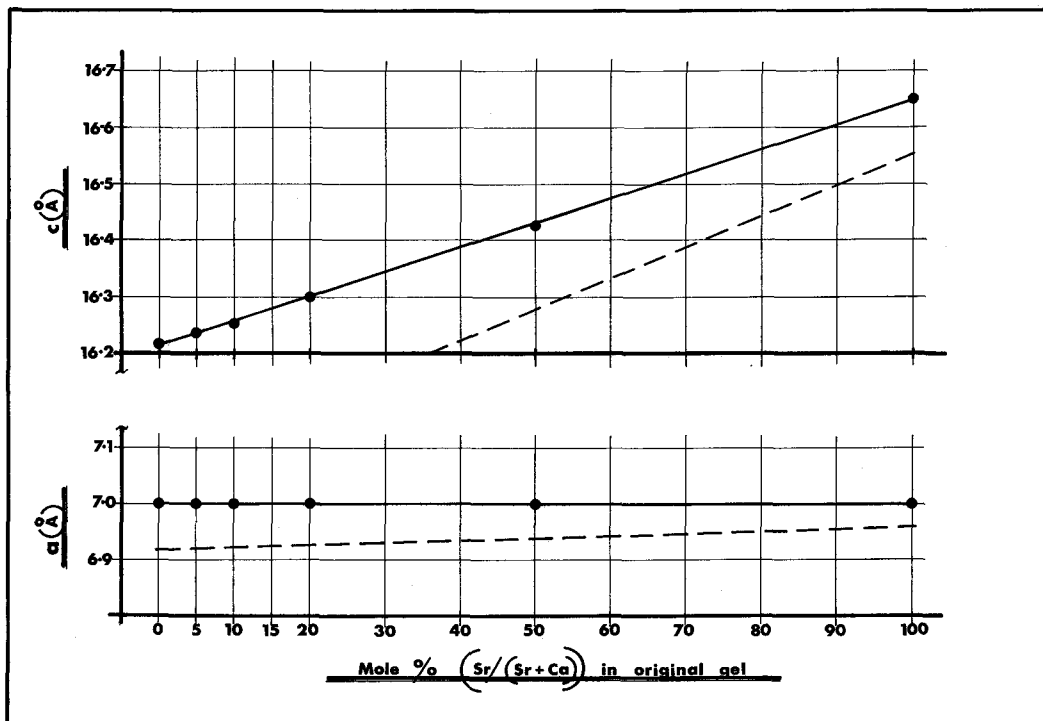


FIG. 1. The relationship between the hexagonal unit cell parameters ( $a$ ,  $c$ , in Å) for members of the synthetic crandallite-goyazite series and the mole % of strontium in the original gel. The broken line is derived from the relationship between cation radius and unit-cell size described by McKie (1962) for naturally occurring members of the plumbogummite group.

octahedra that are parallel to (001) impart rigidity within this plane. In contrast, bonding of these sheets in the  $c$  direction is through weaker hydrogen bonds between the quite distantly opposed  $(\text{OH})_{\frac{1}{2}}\text{O}_{\frac{1}{2}}$  apical anions [O(1) sites of Blount (1974)] of non-linked  $\text{PO}_{3\frac{1}{2}}(\text{OH})_{\frac{1}{2}}$  tetrahedra (i.e. the tetrahedra do not share anions to form rows, sheets, or a framework) and the large 6(OH), 6O [i.e. O(3), O(2) sites] polyhedra surrounding the large cations (Ca, Sr, etc.). Blount (1974) points out that the Ca ion is too small to be equally co-ordinated with all twelve anions, resulting in distortion of the polyhedron and the lack of a preferred position for the Ca ion in the polyhedral cavity. The precise nature of the Ca co-ordination is uncertain since Blount's (1974) refinement of the crandallite structure in space group  $R\bar{3}m$  may be incorrect (Radolovich and Slade, 1980).

Crystal sizes for members of the crandallite-goyazite series were derived from the Scherrer equation (Klug and Alexander, 1962) using measurements of the broadening of 220 and 303 diffraction lines relative to a quartz standard and assuming that broadening was solely due to par-

ticule size (fig. 2). These two reflections gave similar values of mean crystal thickness in different directions within crystals. All Sr-substituted specimens were composed of much smaller crystals ( $c. 250 \text{ \AA}$ ) than the crandallite end-member ( $c. 500 \text{ \AA}$ ).

Particle sizes were also calculated from BET nitrogen adsorption areas, assuming that uniform cubic particles of a single phase were present with a linear variation in density between end-members ( $2.9 \text{ g cm}^{-3}$  for crandallite,  $3.2 \text{ g cm}^{-3}$  for goyazite). These sizes (fig. 2) were similar to those obtained from the Scherrer equation, showing closest agreement for low-Sr specimens, the calculated sizes being about  $50 \text{ \AA}$  bigger for the high-Sr specimens.

*Electron microscopy.* Two morphologically distinct materials occurred in synthetic crandallite; 1–5  $\mu\text{m}$  tapered crystals which were frequently of triangular cross section, and aggregates of platy crystals with individual crystals of approximately  $0.1 \mu\text{m}$  diameter (fig. 3). The tapered crystals commonly grew out of aggregates of platy crystals, the long axes of the tapered crystals being normal to the plates. All Sr-substituted specimens consisted

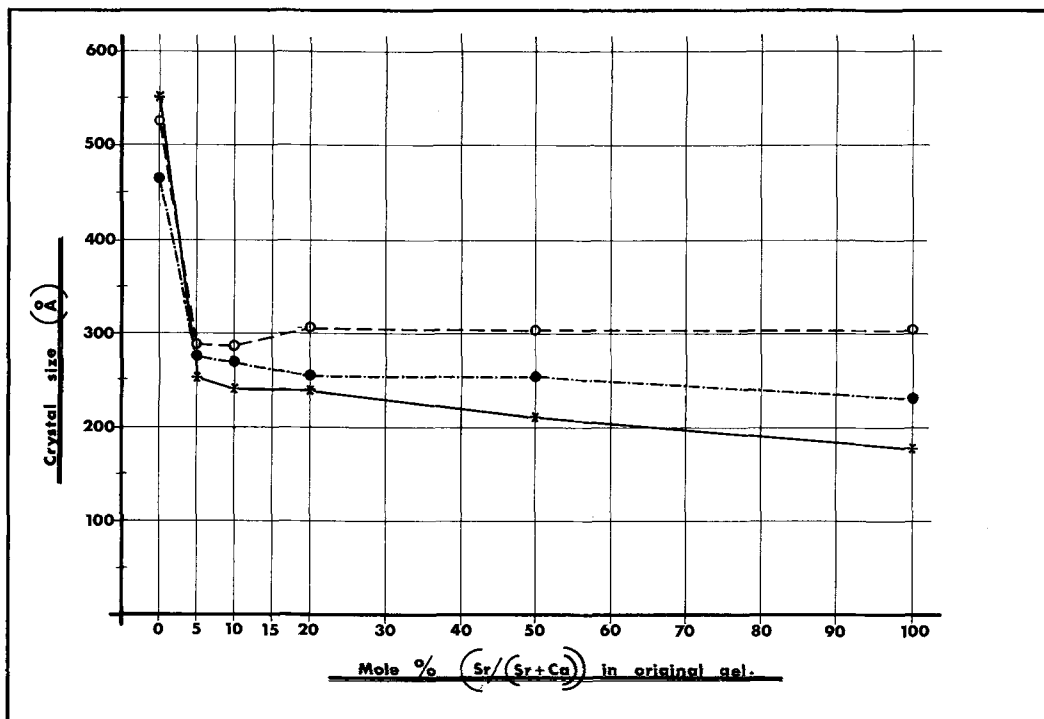


FIG. 2. Crystal sizes of members of the crandallite-goazite series determined from the broadening of the 220 (●) and 303 (\*) diffraction lines and from BET nitrogen adsorption areas (○).

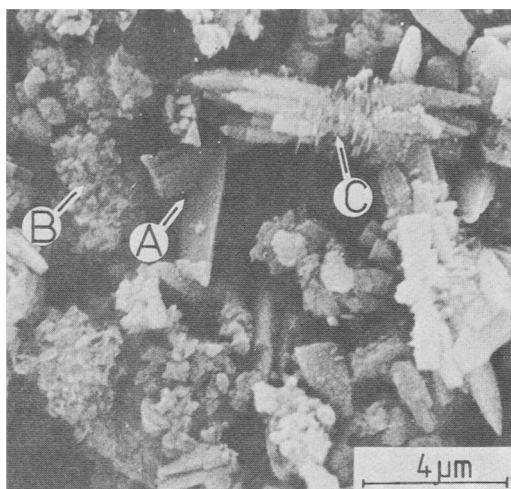


FIG. 3. Scanning electron micrograph of synthetic crandallite showing (A) tapered prismatic crystals, (B) parallel aggregates of platy crystals, and (C) tapered prismatic crystals growing perpendicularly from parallel aggregates of platy crystals.

solely of 0.1  $\mu\text{m}$  platy crystals with occasional subhedral hexagonal shapes.

The typical large tapered crandallite crystal shown in fig. 4 was elongated along its  $c^*$  (i.e.  $c$ ) axis with reflections on the  $a^*$  axis ( $hh2h0$  reflections) occurring in a direction normal to the  $c^*$  axis. The central part of the diffraction pattern consists of reflections of the type  $hh2h3n$ . Thus the  $(1\bar{1}00)$  plane must be approximately perpendicular to the electron beam and nearly parallel to the surface of the Ewald sphere (Gard, 1971). The occurrence of reflections of the type  $h \cdot h + 1 \cdot 2h + 1 \cdot 3n - 1$  in a band that is approximately parallel to the  $a^*$  axis and at distance of  $1.04 \text{ \AA}^{-1}$  from the  $a^*$  axis indicates that the  $(100)$  plane was not exactly perpendicular to the electron beam. The Ewald sphere intercepted the  $(h \cdot h + 1 \cdot 2h + 1 \cdot 3n - 1)$  reciprocal lattice plane which is parallel and adjacent to the  $a^*c^*$  plane and positioned  $0.0825 \text{ \AA}^{-1}$  below it. The reflections in this plane do not fall on the grid defined by the  $a^*c^*$  net because of the systematic extinctions of space group  $R\bar{3}m$ . The points in the adjacent planes are displaced from each other

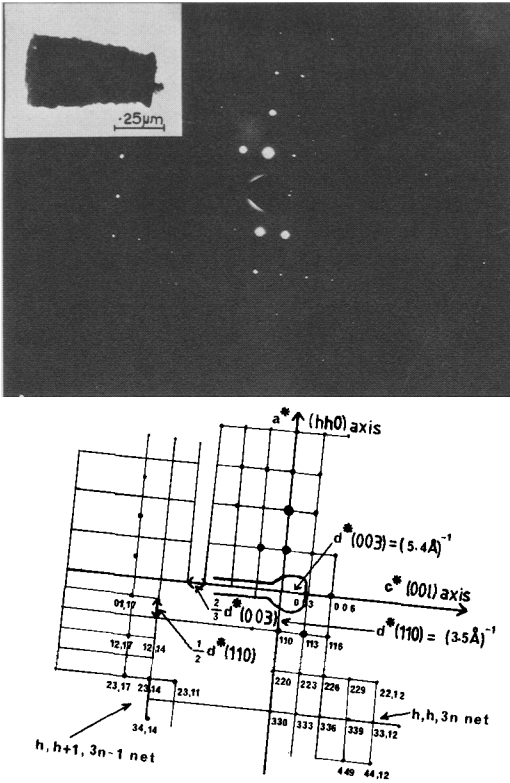


FIG. 4. Transmission electron micrograph and correctly oriented SAD pattern of a tapered prismatic crystal of synthetic crandallite and assignments of reflections to the  $h \cdot h \cdot 2h \cdot 3n$  and  $h \cdot h + 1 \cdot 2h + 1 \cdot 3n - 1$  levels in reciprocal space. The crystal is elongated along its  $c$  axis.

by  $d^*(110)/2$  (i.e.  $0.143 \text{ \AA}^{-1}$ ) in the  $a^*$  direction and  $d^*(003)/3 = d^*(001)$  (i.e.  $0.0617 \text{ \AA}^{-1}$ ) in the  $c^*$  direction as is shown in fig. 4. The  $1.04 \text{ \AA}^{-1}$  separation of bands of reflections from parallel reciprocal lattice planes separated by  $0.0825 \text{ \AA}^{-1}$  indicates that the crystal in fig. 4 was tilted about the  $a^*$  or similar axis by about  $4.5^\circ$ . Most large tapered crystals of synthetic crandallite gave similar SAD patterns. The small platy crystals which were the major component of all specimens were quickly dehydroxylated and contaminated in the electron beam and therefore did not diffract sufficiently strongly to give SAD patterns. However these crystals probably exhibited well developed (001) faces, as do similar but larger crystals in some natural crandallite specimens (Palmer, 1979). This interpretation is consistent with the orientation of the platy crystals normal to the  $c$  axis of those tapered crystals which nucleate from aggregates of platy crystals (fig. 3).

Slade (1974) observed tapered crandallite particles in synthetic crandallite and considered them to be aggregates of acicular crystals whose long axes were perpendicular to the principal axes of the particles. By analogy with the habit of macrocrystalline crandallite from Duchess, Queensland, he argued that the particles consisted of aggregates of very small crystals whose  $a$  axes were parallel to the long axes of the particles and the  $c$  axes radiated out perpendicularly to the long axis. The micron-sized particles of synthetic crandallite depicted in Slade's paper appear to correspond to the tapered crystals investigated in this work which were synthesized according to Slade's procedure. If this is the case, the orientation of  $a$  and  $c$  axes within Slade's particles are the reverse of those postulated by that author. Radiating spherical aggregates of much larger acicular crandallite crystals have been described by Mitchell and Knowlton (1971) and Palache *et al.* (1951) from

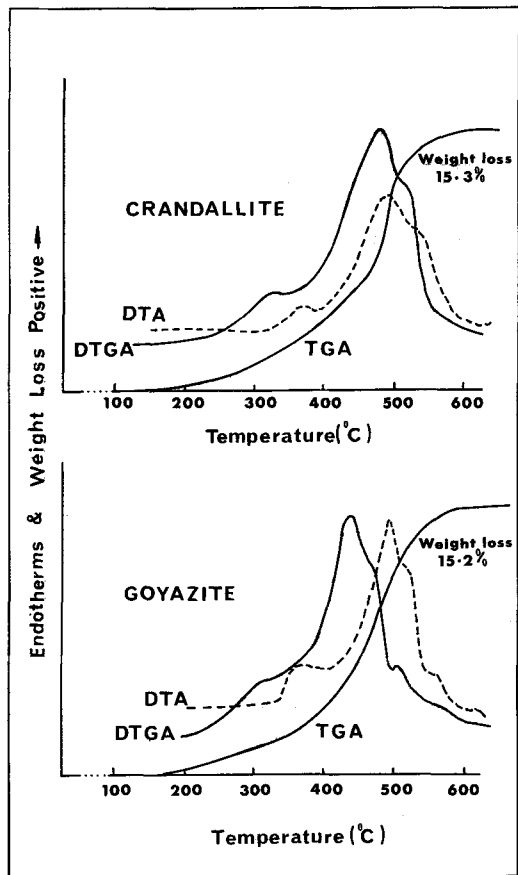


FIG. 5. DTA, TGA, and DTGA curves for crandallite and goyazite.

natural occurrences. The identification of axes agrees with that of Slade (1974), but the very different sizes of natural and synthetic crystals prevent direct comparison and point out the need for an electron optical examination of fragments of these natural macrocrystalline specimens.

*Thermal analysis.* Dehydroxylation temperatures for crandallite-goyazite and the impurity boehmite were systematically higher for DTA measurements than for DTGA measurements. This displacement was probably due to the much larger volume of the DTA samples which reduced the rate at which evolved water diffused from the specimen (Mackenzie, 1970) (fig. 5). For all specimens two dehydroxylation endotherms occurred, a minor one at about 320°C, associated with loss of about 15% of the structural water, and a major endotherm at about 440°C where the remaining water was lost. These losses correspond to half a molecule and three molecules respectively of the total 3.5 molecules per formula unit and might be due to hydroxyls in discrete structural sites. Furthermore, the stronger endotherm and associated DTGA peak had an unresolved high-temperature shoulder that may also correspond to loss of hydroxyls from a distinct structural site.

The weak endotherm at about 550°C for goyazite was due to the boehmite impurity.

Dehydroxylation temperatures decreased with increasing Sr content up to Cr<sub>80</sub>Go<sub>20</sub> and then increased for higher Sr contents (fig. 6). The larger crystal size of the crandallite specimen may have caused its dehydroxylation temperature to be higher and not directly comparable with the other specimens which were more nearly uniform in size. These results are generally consistent with the data for naturally occurring members of the crandallite-goyazite series (Table I) which, despite the wide range in dehydroxylation temperature reported for each mineral, are lowest for specimens with compositions near to that of crandallite. Boehmite crystals were larger in the high-Sr preparations, which resulted in a higher dehydroxylation temperature for this mineral (Mackenzie, 1970).

Subsamples of synthetic crandallite were heated for six hours in a muffle furnace at various temperatures between 250 and 600°C and then examined by XRD. Some (about 6%) crandallite persisted at temperatures up to 500°C although most (about 80%) had dehydroxylated at 450°C to give an amorphous residue. Accurate unit-cell parameters were calculated by regression using twenty-three

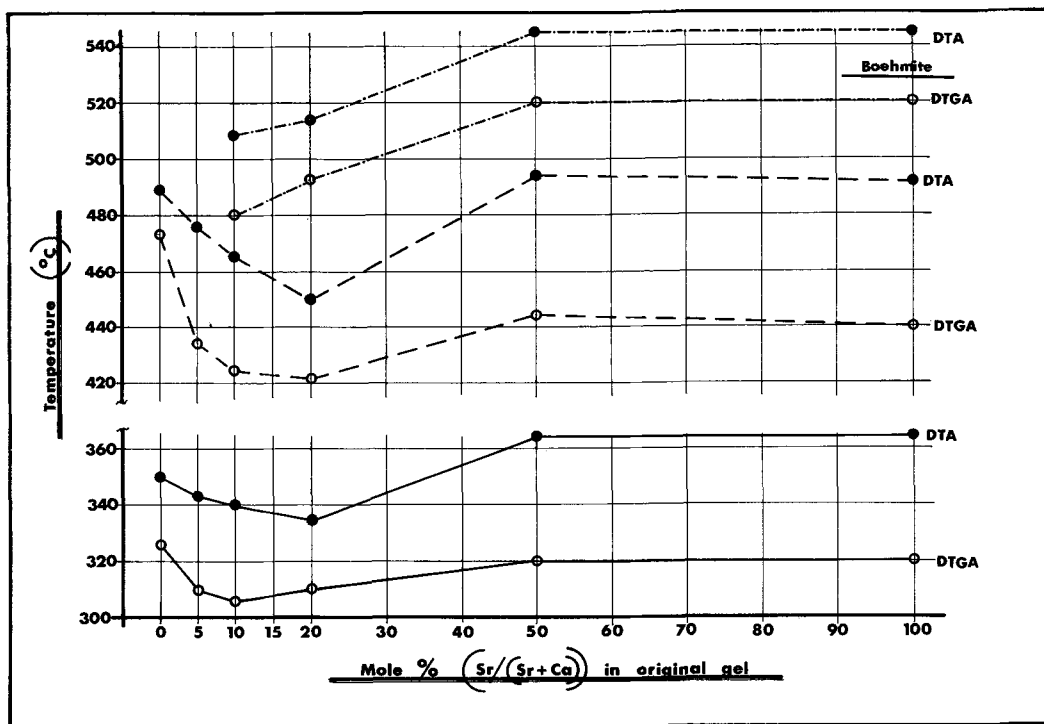


Fig. 6. The relationship between temperature of dehydroxylation peaks measured by DTA (●) and DTGA (○) and the mole % strontium in the original gel. The highest temperature DTA and DTGA data are for the boehmite impurity.

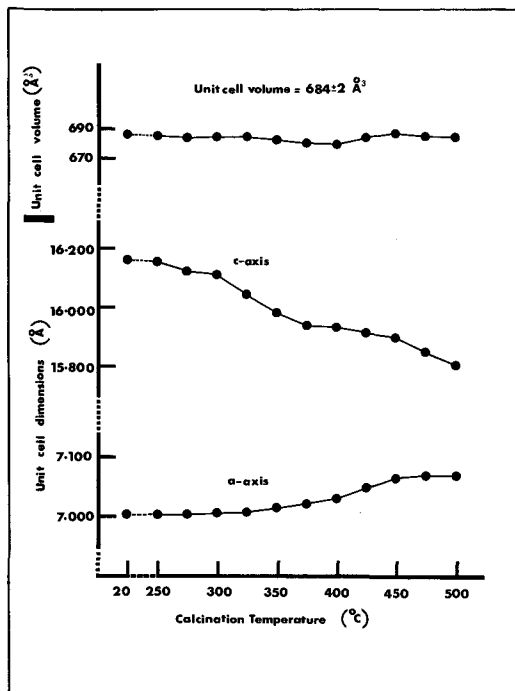


FIG. 7. The relationship between the  $a$  and  $c$  parameters of the unit cell, the unit-cell volume, and calcination temperature for synthetic crandallite.

reflections. The relationship between the  $a$  and  $c$  parameters of the unit cell, the unit-cell volume, and the calcination temperature are shown in fig. 7. Over this temperature range there was a 2.2% decrease in the length of the  $c$  axis and a 0.9% increase in the length of the  $a$  axis, maintaining an almost constant unit cell volume of  $684 \pm 2 \text{ \AA}^3$ . The intensities of all reflections decreased with increasing calcination temperature and the widths of reflections increased, with the 006 reflection exhibiting the greatest broadening.

The much greater change in the  $c$  direction is consistent with the greater sensitivity of this dimension to Sr-substitution as was discussed earlier. The rigidity of the sheets of  $\text{Al}(\text{OH})_4\text{O}_2$  octahedra may be responsible for the structural reorganization of partially dehydroxylated crandallite being mostly accommodated by contraction in the  $c$  direction.

## REFERENCES

- Ankinowitch, E. A., and Silantjewa, N. I. (1959) *Izv. Akad. Nauk Kazakh. SSR, ser. geol.* **36**, 78–81.
- Blanchard, F. N. (1972) *Q. J. Fla. Acad. Sci.* **34**, 1–9.
- Blount, A. M. (1974) *Am. Mineral.* **59**, 41–7.
- Cowgill, U. M., Hutchinson, G. E., and Joensuu, O. (1963) *Ibid.* **48**, 1144–53.
- Doak, B. W., Gallaher, P. J., Evans, L., and Muller, F. B. (1965) *N. Z. J. Agric. Res.* **8**, 15–29.
- Gard, J. A., ed. (1971) *The electron-optical investigation of clays*, Mineralogical Society, London.
- Gilkes, R. J., and Palmer, B. (1979) *Aust. J. Soil Res.* **17**, 467–81.
- Guillemin, J. (1955) *Bull. Soc. fr. Mineral. Cristallogr.* **78**, 27–32.
- Hill, W. L., Armiger, W. H., and Gooch, S. D. (1950) *Trans. Am. Inst. Min. (Metall.) Eng.* **187**, 699–702.
- Hoare, J. (1980) In *The Role of Phosphorus in Agriculture* (Khasawneh, F. E. et al., eds.) Madison, Wisconsin, American Soc. Agron. 121–7.
- Ignatova, L. I., Karpova, L. N., and Zhil'tozova, I. G. (1965) *Geokhimiya*, **18**, 1355–9.
- Kato, T., and Radoslovich, E. W. (1968) *Trans. 9th Congr. Int. Soil Sci. Soc., Adelaide*, **2**, 725–31.
- Klug, H. P., and Alexander, L. E. (1962) *X-ray Diffraction Procedures*. John Wiley, New York.
- Mackenzie, R. C., ed. (1970) *Differential Thermal Analysis*, Academic Press, London.
- McKie, D. (1962) *Mineral. Mag.* **33**, 281–97.
- Mitchell, R. S., and Knowlton, S. M. (1971) *Mineral. Rec.* **2**, 223–4.
- Nicolas, J., and de Rosen, A. (1963) *Bull. Soc. fr. Mineral. Cristallogr.* **86**, 379–85.
- Norrish, K. (1968) *Trans. 9th Congr. Int. Soil Sci. Soc., Adelaide*, **2**, 713–23.
- Palache, C., Berman, H., and Frondel, C. (1951) *Dana's System of Mineralogy*, **2**, 834–7. John Wiley, New York.
- Palmer, B. (1979) *A chemical, mineralogical and biological evaluation of Christmas Island C-grade rock phosphate*. Ph.D. thesis, University of Western Australia.
- Povondra, P., and Slansky, E. (1966) *Acta Univ. Carolinae, Geol.* **1**, 61–76.
- Radoslovich, E. W. (1969) *CSIRO Australia, Div. Soils Tech. Memo 10*.
- and Slade, P. G. (1980) *Neues Jahrb. Mineral. Mh.* 157–70.
- Rao, A. B. (1966) *Mineral. Mag.* **35**, 427–8.
- Slade, P. G. (1974) *Neues Jahrb. Mineral. Mh.* 22–7.

[Manuscript received 18 March 1982;  
revised 30 July 1982]